

What is Missing from the Local Stellar Halo?

KATHERINE SHARPE ¹, ROHAN P. NAIDU ^{1,2,*} AND CHARLIE CONROY ¹

¹Center for Astrophysics — Harvard & Smithsonian, 60 Garden Street, Cambridge, MA 02138, USA

²MIT Kavli Institute for Astrophysics and Space Research, 77 Massachusetts Avenue, Cambridge, MA 02139, USA

ABSTRACT

The Milky Way’s stellar halo, which extends to > 100 kpc, encodes the evolutionary history of our Galaxy. However, most studies of the halo to date have been limited to within a few kpc of the Sun. Here, we characterize differences between this local halo and the stellar halo in its entirety. We construct a composite stellar halo model by combining observationally motivated N-body simulations of the Milky Way’s nine most massive disrupted dwarf galaxies that account for almost all of the mass in the halo. We find that (1) the representation by mass of different dwarf galaxies in the local halo compared to the whole halo can be significantly overestimated (e.g., the Helmi Streams) or underestimated (e.g., Cetus) and (2) properties of the overall halo (e.g., net rotation) inferred via orbit integration of local halo stars are significantly biased, because e.g., highly retrograde debris from Gaia-Sausage-Enceladus is missing from the local halo. Therefore, extrapolations from the local to the global halo should be treated with caution. From analysis of a sample of 11 MW-like simulated halos, we identify a population of recently accreted ($\lesssim 5$ Gyrs) and disrupted galaxies on high angular momenta orbits that are entirely missing from local samples, and awaiting discovery in the outer halo. Our results motivate the need for surveys of halo stars extending to the Galaxy’s virial radius.

Keywords: Galaxy: halo — Galaxy: formation

1. INTRODUCTION

In Λ CDM cosmology, galaxies grow hierarchically, with smaller systems continuously merging into more massive galaxies (e.g., White & Frenk 1991). Our clearest view into this hierarchical assimilation comes from the stellar halo of the Milky Way, which is almost entirely comprised of debris from accretion events (e.g., Di Matteo et al. 2019; Mackereth & Bovy 2020; Naidu et al. 2020). Families of halo stars that arrived as part of the same galaxy retain similar phase space properties (e.g., energies, angular momenta, actions; Brown et al. 2005; Gómez et al. 2013; Simpson et al. 2019) as well as shared chemical abundance patterns (e.g., Lee et al. 2015; Cunningham et al. 2022). With detailed chemodynamical data, it is challenging (e.g., Jean-Baptiste et al. 2017) but possible to determine which populations of stars were originally associated with the same dwarf galaxy merger event. From satellite galaxies being currently disrupted (e.g., Sagittarius; Ibata et al. 1994) to stellar populations fully integrated into the halo (e.g., Thamnos; Koppelman et al. 2019), dwarf galaxies in all stages

of accretion can be found in and around the stellar halo, encoding our Galaxy’s assembly history.

The stellar halo is difficult to study directly due to its small relative mass ($\approx 1\%$ of the Galaxy’s stellar mass; Deason et al. 2019), large spatial extent, and the necessity to collect full 6D phase-space and abundance data to reconstruct its history with high fidelity. Thanks to numerous spectroscopic surveys (e.g., RAVE, Steinmetz et al. 2006; SEGUE, Yanny et al. 2009; LAMOST, Cui et al. 2012; GALAH, De Silva et al. 2015; APOGEE, Majewski et al. 2017; H3, Conroy et al. 2019; and the *Gaia* mission, Gaia Collaboration et al. 2018), we have detailed chemodynamical parameters for thousands of stars in the stellar halo. However, owing to observational feasibility, the vast majority of halo stars studied in depth are located in the solar neighborhood, within a few kiloparsecs of the Sun (the “local halo”).

From the local halo, it is possible to infer the properties of the more distant halo. An important technique is integrating local halo stars’ orbits and analyzing their properties based on their orbital apocenters, which is the maximum distance they reach from the Galactic center. This method is, for example, applied to determine the net rotation of the outer halo, which may provide evidence as to its method of formation (e.g., Carollo et al.

ksharpe@college.harvard.edu, rnaidu@mit.edu

* NASA Hubble Fellow

2007; Schönrich et al. 2011; Beers et al. 2012; Helmi et al. 2017).

However, we know that the local halo is unrepresentative of the stellar halo in its entirety. For instance, stars associated with the prominent dwarf galaxies Cetus (e.g., Newberg et al. 2009) and Sagittarius are not found within the solar neighborhood; thus, any extrapolations from local samples cannot capture any information about these two accreted dwarf galaxies. Apocenter analyses do not accurately capture the more radially extreme stars in an accreted dwarf. Accreted stars are most likely to be found close to their apocenters (e.g., Deason et al. 2018), meaning stars on large-apocenter orbits are least likely to be found near the Sun. Additionally, there is a degree of selection bias when determining which stars within the solar neighborhood actually belong to the stellar halo and which are associated with the Galactic disk (e.g., stars that are retrograde with respect to the disk are more likely to be classified as halo stars).

In this paper, we aim to precisely determine what differences might exist between extrapolations from the local halo and the stellar halo as a whole. We begin by constructing a composite model of the Milky Way’s stellar halo, described in Section 2 and Section 3.1. Then, in Section 3.2, we study the relative representation of stars in the local halo compared to the stellar halo in its entirety for all accreted dwarfs in the composite model. We also perform apocenter analysis, after integrating the orbits of local halo stars, to compare apocenter properties to those of whole halo stars, focusing on net prograde/retrograde motion. In Section 3.3, we compare the composite halo with the eleven halo simulations from Bullock & Johnston (2005); Robertson et al. (2005); Font et al. (2006) (hereafter BJ05). Finally, in Section 4 we summarize our conclusions and present a few final remarks.

2. METHOD

2.1. *Simulation Sources*

In this section, we describe how our composite Milky Way stellar halo is constructed, as well as the set of simulations from BJ05 we use to place the composite model in context.

We assemble a composite Milky Way stellar halo from observationally motivated simulations representing nine accreted dwarf galaxies: Gaia-Sausage-Enceladus (GSE, e.g., Belokurov et al. 2018; Haywood et al. 2018; Helmi et al. 2018; Bonaca et al. 2020; Feuillet et al. 2021; Naidu et al. 2021; Buder et al. 2022), Sagittarius (e.g., Ibata et al. 1994; Law & Majewski 2010; Johnson et al. 2020; Vasiliev et al. 2021), Kraken (Kruijssen et al. 2019, 2020; Massari et al. 2019; Forbes 2020; Horta et al. 2021; Pfeffer et al. 2021; Naidu et al. 2022b; though note that the stars and clusters associated with Kraken

may belong to the proto-Milky Way recently characterized in Belokurov & Kravtsov 2022; Conroy et al. 2022; Myeong et al. 2022; Rix et al. 2022), the Helmi Streams (e.g., Helmi et al. 1999; Koppelman et al. 2019; Limberg et al. 2021; Matsuno et al. 2022), Sequoia (e.g., Myeong et al. 2019; Matsuno et al. 2019, 2021; Monty et al. 2020; Aguado et al. 2021), Wukong/LMS-1 (hereafter Wukong, e.g., Naidu et al. 2020; Yuan et al. 2020; Malhan et al. 2021, 2022; Shank et al. 2022), Cetus (e.g., Newberg et al. 2009; Chang et al. 2020; Thomas & Battaglia 2021; Yuan et al. 2021), Thamnos (e.g., Koppelman et al. 2019; Sofie Lövdal et al. 2022; Ruiz-Lara et al. 2022), and I’itoi (e.g., Naidu et al. 2020, 2022a). These nine systems together comprise almost all known $M_* \gtrsim 10^6 M_\odot$ accreted systems, and nearly all of the total stellar halo ($\approx 10^9 M_\odot$, Deason et al. 2019) by mass (see Table 1 of Naidu et al. 2022a for stellar mass estimates of individual dwarfs). Models of these systems therefore provide a realistic approximation of the Milky Way for the issues we are interested in.

We note that several lower mass ($< 10^6 M_\odot$) dwarf galaxies (e.g., Shipp et al. 2018; Ji et al. 2020; Bonaca et al. 2021; Tenachi et al. 2022; Dodd et al. 2022; Chandra et al. 2022) are predicted (e.g., Robertson et al. 2005; Deason et al. 2016; Fattahi et al. 2019) and observed (e.g., Naidu et al. 2020; Helmi 2020; An & Beers 2021) to contribute a small minority of the stellar halo. While we do not include such systems in our composite Milky Way model, they are captured in the BJ05 simulated halos we analyze, and the general trends we report apply to them.

We use star particles from five tailor-made N-body simulations, representing GSE (Naidu et al. 2021), Sagittarius (Vasiliev et al. 2021), the Helmi Streams (Koppelman et al. 2019), Wukong/LMS-1 (hereafter Wukong, Malhan et al. 2021), and Cetus (Yuan et al. 2021). We note that for Sagittarius, we cut out the intact core and keep the remaining $\approx 3 \times 10^8 M_\odot$ found within the disrupted tails. However, Sagittarius is shown in its entirety as a part of Figures 1 and 2.

Four of the dwarfs we consider — Kraken, Sequoia, Thamnos, and I’itoi — have not yet had dedicated simulations run. We select representative models for these four objects from the simulated dwarf galaxies in the halos from BJ05 on the basis of similarities in phase and real space. We begin by selecting the sample of dwarfs from BJ05 with similar total mass, average z-component angular momentum (L_z), and total energy to each of the four dwarfs. We then visually compare the $L_z - E_{\text{tot}}$ to observational data. Where multiple simulations had comparable phase space distributions, similarities in average galactic radius were also considered.

Later in the paper (Section 3.3) we also compare the eleven BJ05 simulated halos in their entirety to our composite Milky Way stellar halo. These halos follow cosmologically motivated accretion histories for Milky Way

Table 1. Summary of Accreted Dwarf Galaxies in the Milky Way Stellar Halo Composite Model.

Dwarf Galaxy	$\log(M_*/M_\odot)$	N_*	Mass per Particle (M_\odot)	Time Unbound (Gyr)	Simulation Source
Sagittarius	8.5 (8.8)	200,000	3,155	0	Vasiliev et al. (2021)
GSE	8.7	50,060	9,988	9	Naidu et al. (2021)
Kraken	8.3	3,002	63,291	12	BJ05: Halo 3, ID 91
Helmi Streams	8.0	100,000	1000	5-8 (6.5)	Koppelman et al. (2019)
Sequoia	7.2	12,512	1,267	7	BJ05: Halo 1, ID 51
Wukong/LMS-1	7.1	15,580	808	8	Malhan et al. (2021)
Cetus	7.0	200,000	50	5	Chang et al. (2020)
Thamnos	6.7	10,256	489	11	BJ05: Halo 6, ID 66
I'toi	6.3	2,645	754	10	BJ05: Halo 4, ID 75

NOTE—Objects are listed in order of decreasing total stellar mass. Stellar masses are sourced from Naidu et al. (2022a) for all objects except for Kraken, for which we use Kruijssen et al. (2020). The total stellar mass of Sagittarius is shown in the parenthesis; we cut approximately $3 \times 10^8 M_\odot$ about the center of the Sagittarius dwarf galaxy as it is often considered separately from analysis of the stellar halo. N_* is the number of particles from each simulation. Due to differences in simulation resolution for these nine objects, we weight our analysis on the mass per particle (the total stellar mass of each dwarf galaxy divided by the number of particles in its N-body simulation). We include the “time unbound”, representing the disruption epoch for each dwarf galaxy when it ceased to be a gravitationally bound object. For the stated range on the Helmi Stream’s time unbound, we adopt the median of the range reported in Koppelman et al. (2019). For Kraken, Sequoia, Thamnos, and I’toi, simulations are selected from BJ05 based on similarities in L_z , total energy, and 3D Galactocentric distance.

mass galaxies. Each halo has on the order of 100 accreted dwarf galaxies.

The key properties of the individual simulations comprising the composite Milky Way halo are summarized in Table 1. To account for the differences in resolution between simulations, we weight each particle by distributing the total stellar mass of each accreted dwarf galaxy evenly across all of the simulation’s N particles (see “Mass per Particle” in Table 1).

2.2. Dynamical Properties and Orbit Integration

We integrate orbits for our composite stellar halo particles in the default `gala` Milky Way gravitational potential (Price-Whelan et al. 2018). This potential consists of a spherical nucleus and bulge, a disk, and a spherical dark matter halo (Bovy 2015). For the additional eleven halo simulations, halo parameters reported in BJ05 are implemented via `gala`’s composite potential functionality. Due to the differences between our adopted fiducial Milky Way potential and the potentials for the BJ05 simulations, the four simulated dwarfs selected to represent Thamnos, Sequoia, I’toi, and Kraken are rescaled to retain their approximate positions in phase space — all particle velocities are scaled by the ratio of the circular velocities at their average radius in the Milky Way potential to that of their BJ05 potential ($v_{\text{circ,MW}}/v_{\text{circ,BJ05}}$).

We use the default Galactocentric frame from `Astropy` v4.2.1. This frame is right-handed, and the origin is placed at the galactic center. Prograde motion is represented by a negative z -component of angular momentum ($L_z < 0$). Orbit integrations are performed on stars within the solar neighborhood via `gala`. The orbits of all stars in the solar neighborhood are integrated for-

ward by 5 Gyr. This replicates how the outer halo is often explored in the literature via local halo samples (e.g., Carollo et al. 2007).

3. RESULTS

3.1. Overview of the Composite Milky Way Stellar Halo

The analysis in this paper centers around the composite simulated Milky Way stellar halo described in Section 2.1. We display this composite halo as a projection onto the XY and XZ planes in Figures 1 and 2, respectively. Each of the simulated dwarfs are shown in color in a mini-panel surrounding the composite view. Simulations selected from BJ05 are located along the right.

We observe three types of distributions for these simulated dwarfs. In order of increasing relaxation: (1) stream-like, including Sagittarius and Cetus; (2) spheroidal, including GSE, the Helmi Streams, Sequoia, Wukong, and I’toi; and (3) compact spheroidal or flattened, including Kraken and Thamnos. Based on this figure, it appears that the solar neighborhood is most likely to represent stars from spheroidal-type dwarfs, due to their more homogeneous distribution. Likewise, stream-like dwarfs and the most compact of the spheroidal dwarfs are most likely to be absent from the solar neighborhood, since their physical extent does not intersect the position of the Sun.

We quantitatively explore the relative representation of accreted dwarfs in the local halo in Section 3.2, and study their angular momenta distributions in Section 3.3.

3.2. Examining Bias in the Local Halo

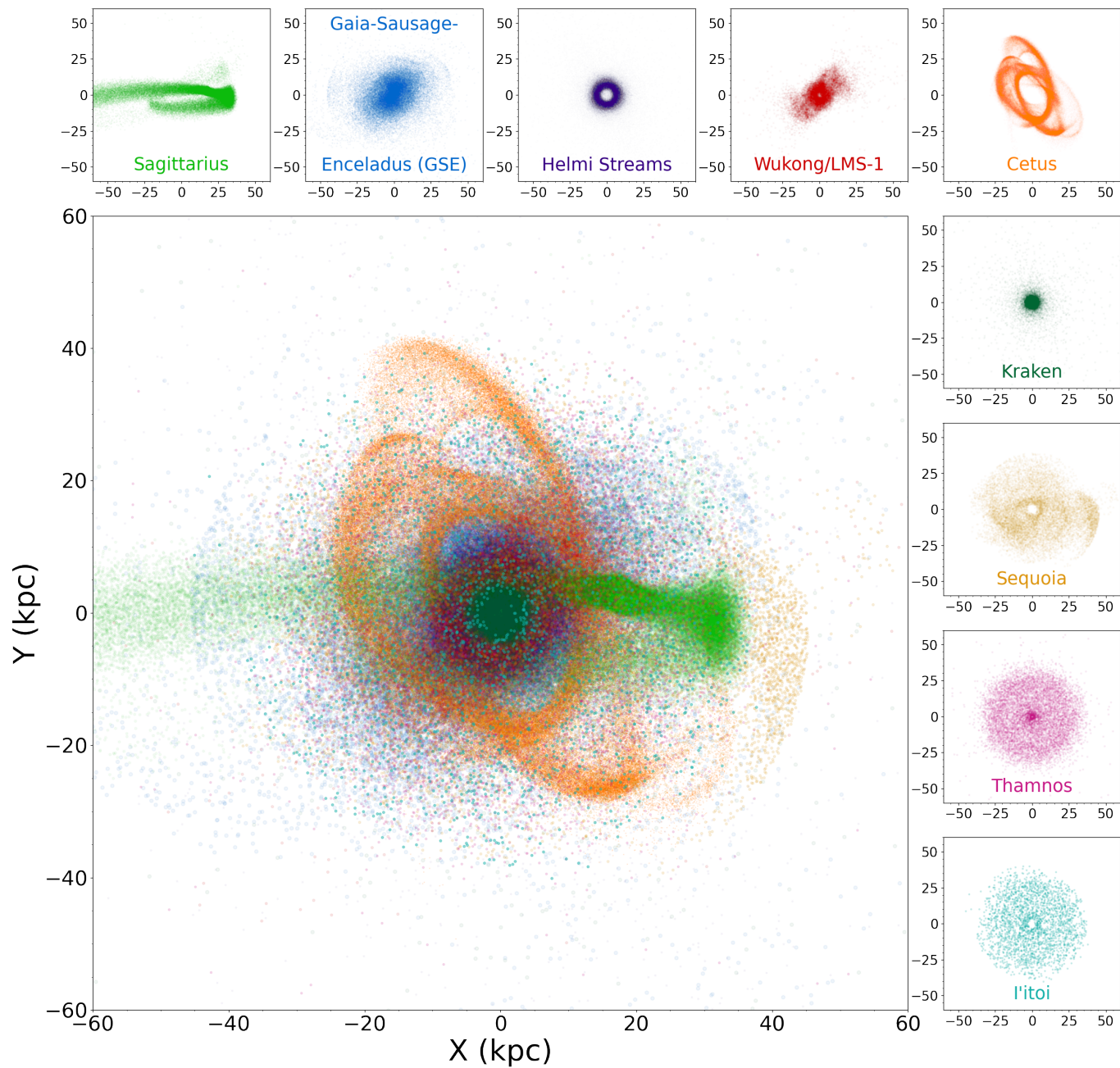


Figure 1. Composite Milky Way stellar halo, displayed in the XY plane. Each accreted dwarf galaxy is shown in color as its own panel and in the large, composite panel. The four panels directly to the right of the large composite plot are those selected from BJ05. In the large panel, point size and opacity are roughly scaled to the power $3/4$ and $1/3$ of mass per particle, respectively, with slight scaling variations for visual clarity.

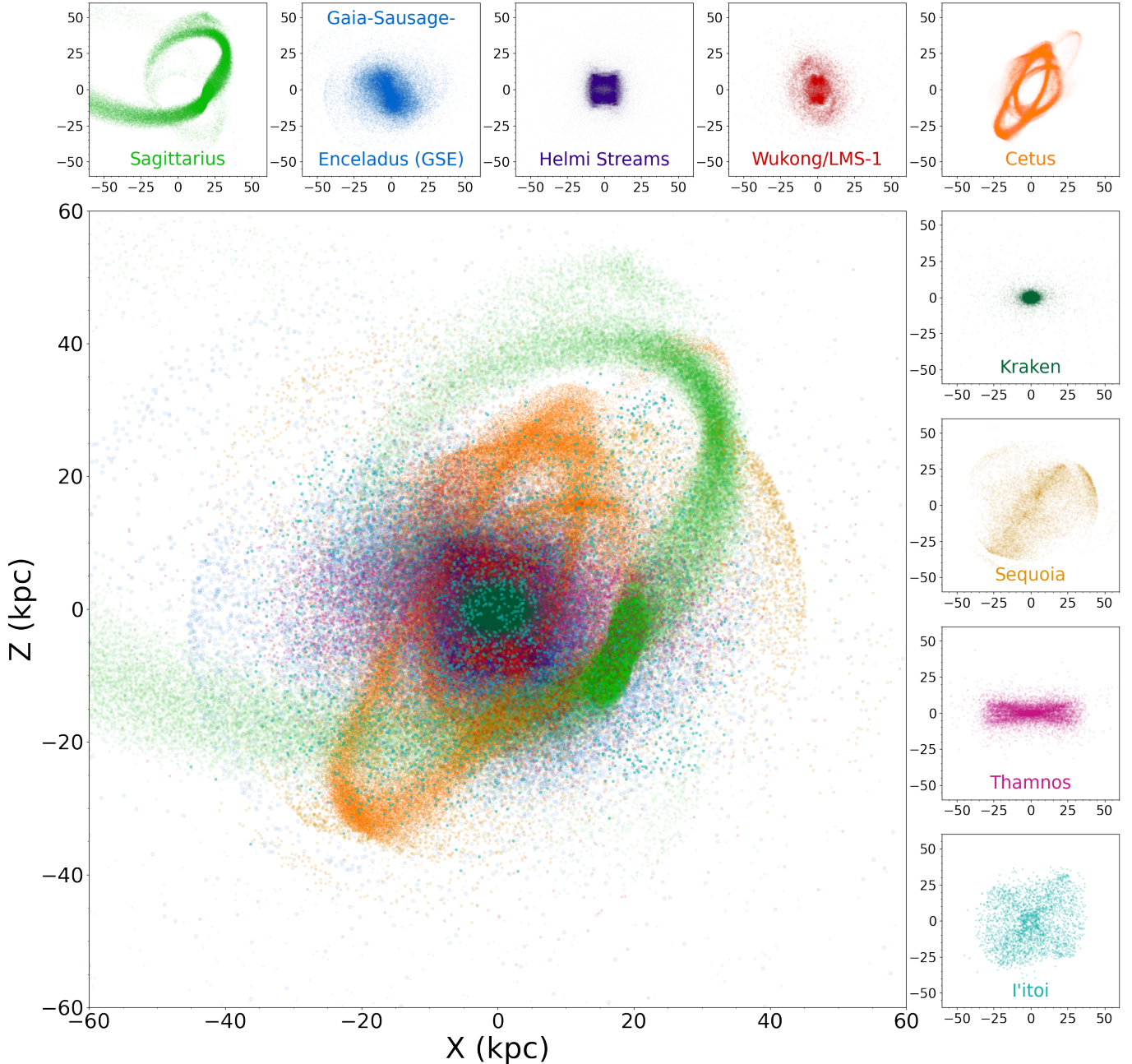


Figure 2. Composite Milky Way stellar halo, displayed in the XZ plane. See caption of Figure 1.

We begin our analysis by considering to what degree each accreted dwarf galaxy is represented within the local halo sample. In an unbiased sample, we expect the relative representation of each accreted dwarf by mass to approximately equal its whole halo mass fraction.

In Figure 3, we compare the mass fractions of each dwarf galaxy within the local halo to those of the whole halo. This comparison is made for local halo with radii 3 kpc (left), and 10 kpc (right). Equal representation between the local halo and the whole halo falls along the central gray 1:1 line. Cetus and Sagittarius are absent

in the 3 kpc local halo, and are shown as arrows pointing towards zero.

Representation within the local halo does not approximate the mass fraction of each of the composite halo dwarf galaxy sources. For example, both Cetus and Sagittarius are completely unrepresented in the 3 kpc local halo, and are still under-represented in the 10 kpc local halo. Additionally, I'toi and Sequoia are under-represented by more than a factor of two. Meanwhile, Kraken is over-represented in the 3 kpc local halo by more than a factor of two — this over-representation is increased in the 10 kpc local halo as the solar neigh-

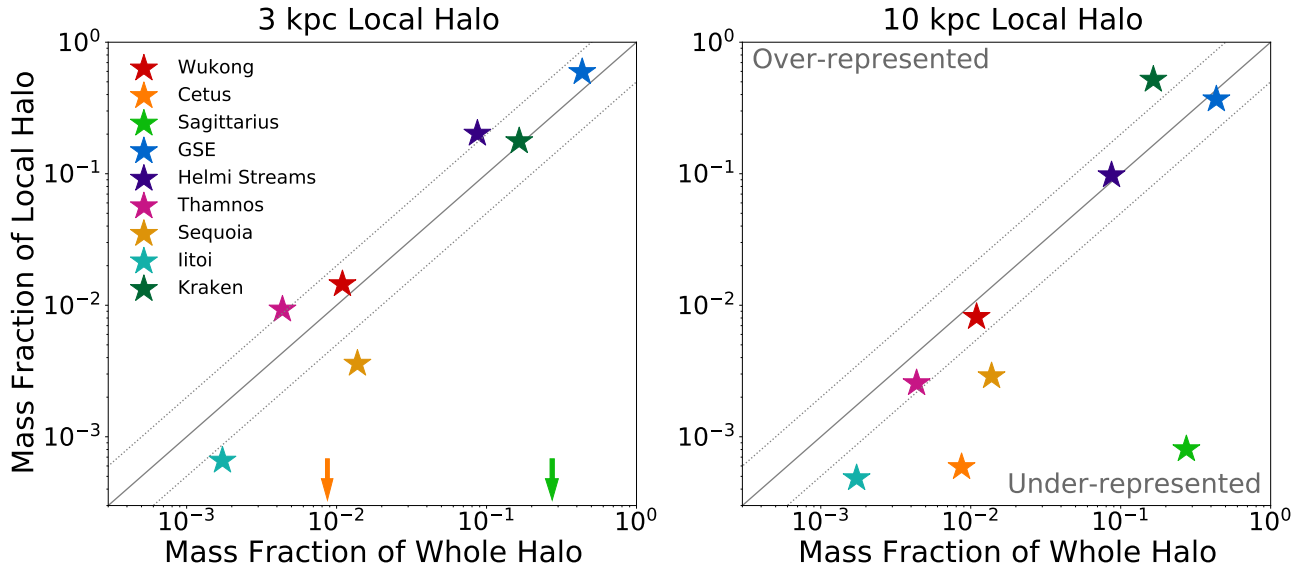


Figure 3. Comparison of the fractional composition of the whole halo to that of the local halo for each object. The left panel shows this comparison for a local halo with radius 3 kpc, while the right shows the same for an extended local halo with radius 10 kpc. The central gray line is where all points would fall if representations were equal between the local halo and the whole halo. The upper and lower gray dashed lines show a local halo representation $2\times$ and $0.5\times$ the representation of the whole halo, respectively. Note that the two entirely unrepresented objects with a local halo fraction of zero, Cetus and Sagittarius, are shown as upper limits, and that the above plots are in log scale.

borhood then includes the galactic center. Note that in practice, it can be extremely challenging to probe the halo around the Galactic center due to extinction. This situation is changing rapidly thanks to *Gaia* – for instance, Rix et al. (2022) recently used the low-resolution XP spectra from DR3 to reveal a metal poor population which is very compact around the Galactic center.

Now, we examine the properties of local halo stars at their apocenters. In the literature, apocenter analysis is used to extrapolate observations of the local halo to the distant halo — local halo stars are taken to be distant stars on an interior part of their orbit. However, there are some challenges associated with this type of analysis. Even in a homogeneous stellar halo, it is more difficult to capture stars with large apocenters in a local halo sample — these stars spend much of their orbits at large radii, and thus are unlikely to be found near the Sun.

In the upper panel of Figure 4, we show the relative amount of stellar mass at each radius approximated based on apocenters of local halo stars. We also show GSE, the stellar halo without Sagittarius, and the stellar halo in its entirety. We show non-Sagittarius halo stars since Sagittarius is the most massive component beyond about 30 kpc, and it is useful to see to what degree the results depend on this one dwarf. Similarly, GSE dominates the local halo, and it is interesting to isolate its effect.

The most striking feature in the upper panel of Figure 4 is that local halo stars are selectively probing 10 – 15 kpc. This peak corresponds to the final apocenter of the GSE galaxy before it was entirely disrupted in

the Naidu et al. (2021) simulations. This prediction has been recently confirmed by the H3 Survey (Han et al. 2022). Another key feature is that stars beyond about 20 kpc (the “outer halo”) are very sparsely represented in the local halo relative to their true distribution.

The lower panel of Figure 4 shows the relative amount of stellar mass as a function of L_z in the outer halo beyond 20 kpc. A large prograde component from Sagittarius is present in the whole halo which is missing from the local halo. Local halo stars are much more radial than the entire halo; i.e., very small values of L_z are over-represented. This is because, analogous to the Sagittarius dwarf galaxy, stars with higher angular momenta from other dwarfs are less likely to pass near the Sun.

We examine the prograde/retrograde motion of the halo in more depth by considering L_z as a function of 3D galactocentric distance, r_{gal} (Figure 5). The whole halo is prograde on average out to 100 kpc, and the magnitude of L_z increases with radius. In the more distant halo, this is due to the contribution from Sagittarius. When we exclude Sagittarius, the net motion in the distant halo is significantly retrograde owing to GSE.

Interestingly, the local halo samples selected from the composite model predict a retrograde outer halo, the magnitude of which is consistent with Carollo et al. (2007, 2010). However, the actual non-Sagittarius halo in the model at these distances is *even more* retrograde. This trend is because the outer-most wraps of GSE at $r_{\text{gal}} \gtrsim 50$ kpc predicted by the Naidu et al. (2021) simulations, and motivated by the “Arjuna” substructure

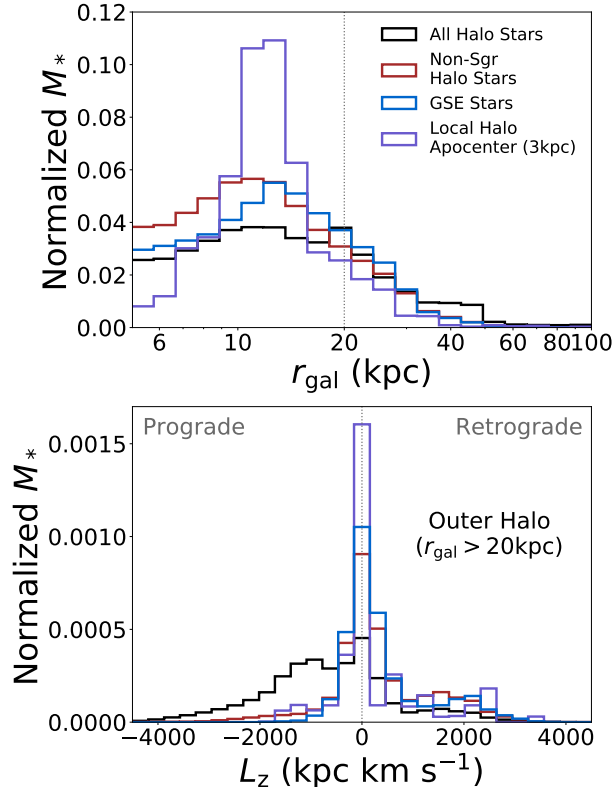


Figure 4. Histograms comparing the properties of the present day whole halo (in black), whole halo without Sagittarius (brown), and GSE (blue) to those of the local halo’s apocenters (for a 3 kpc solar neighborhood in purple). **Top:** The relative stellar mass at each Galactocentric radius. The gray dashed line at 20 kpc denotes the boundary beyond which we classify stars as being in the ‘outer halo’. At radii greater than about 20 kpc, we see a smaller fraction of stars from local halo apocenters when compared to the entire population of halo stars. The local halo’s apocenter distribution peaks at $\approx 15 - 20$ kpc, corresponding to GSE’s inner orbital apocenter (e.g. Naidu et al. 2021; Han et al. 2022). **Bottom:** L_z for local halo stars with apocenters in the outer halo (beyond 20 kpc) to those of the actual halo beyond 20 kpc, using the same color scheme as the upper panel. The local halo is significantly more radial, i.e., concentrated at $L_z \approx 0$ than the actual halo.

associated with GSE (Naidu et al. 2020), are extremely retrograde.

3.3. Comparison to Other Milky Way-like Stellar Halo Simulations

Our composite halo is comprised of simulations representing the nine most massive accreted galaxies which comprise the vast majority of the stellar halo by mass. However, we note that there are several lower mass objects that we do not include in this analysis, which owing to their small halo fractions present only minor pertur-

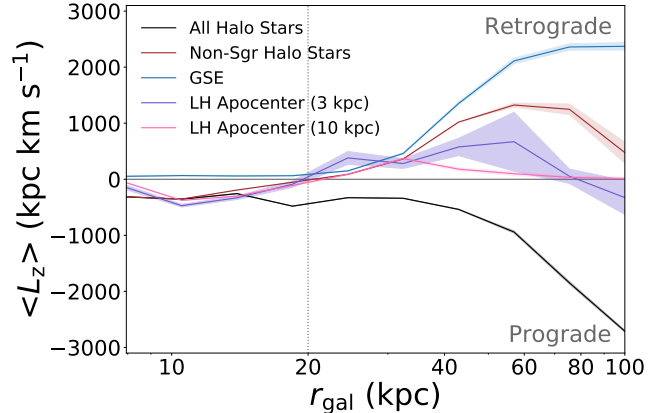


Figure 5. Comparison of the average L_z of all halo stars (in black), halo stars excluding Sagittarius (brown), GSE stars (blue), and local halo apocenters (for a solar neighborhood of 3 kpc in purple). One standard deviation is shaded above and below each line. The gray dotted line marks the beginning of the outer halo (20 kpc). The angular momentum distribution of the outer halo extrapolated from the local halo is significantly more radial than the actual halo.

bations to our findings here. Further, there are likely several disrupted dwarfs that are yet to be discovered (e.g., Fattahi et al. 2020). To explore the full possible parameter space, we compare the nine dwarfs within our composite halo to the $\approx 1,000$ found within the eleven Milky Way-like stellar halos from BJ05.

In Figure 6, we place our composite Milky Way stellar halo in context amongst the eleven BJ05 Milky Way-like stellar halos. Each panel corresponds to a single stellar halo, within which every accreted dwarf galaxy is plotted as a separate circle, with more massive dwarfs being larger. Points are colored as per the fraction of the dwarf’s mass that is represented in the local halo of radius 3 kpc; dwarfs with no stars within the local halo are shown as empty black circles.

The accreted dwarf galaxies in our composite halo, when compared to the halos from BJ05 fall within a similar band of increasing average L_{tot} with decreasing time unbound (the time at which each galaxy ceased to be a gravitationally bound object). Across this band, we see a gradient of representation wherein objects in the bottom right (i.e., high angular momenta, recently accreted objects) are the least likely to be present in the local halo. This pattern is consistent with Sagittarius and Cetus in our composite halo.

These trends excitingly imply that there is a large population of recently accreted disrupted dwarfs (empty circles in Figure 6) with high angular momenta orbiting almost exclusively at large distances which are yet to be discovered. These galaxies are predominantly low-mass systems, relatively unmixed, and present as coherent streams at $\gtrsim 50$ kpc that promise to provide exquisite constraints on the mass distribution (e.g., Bonaca et al.

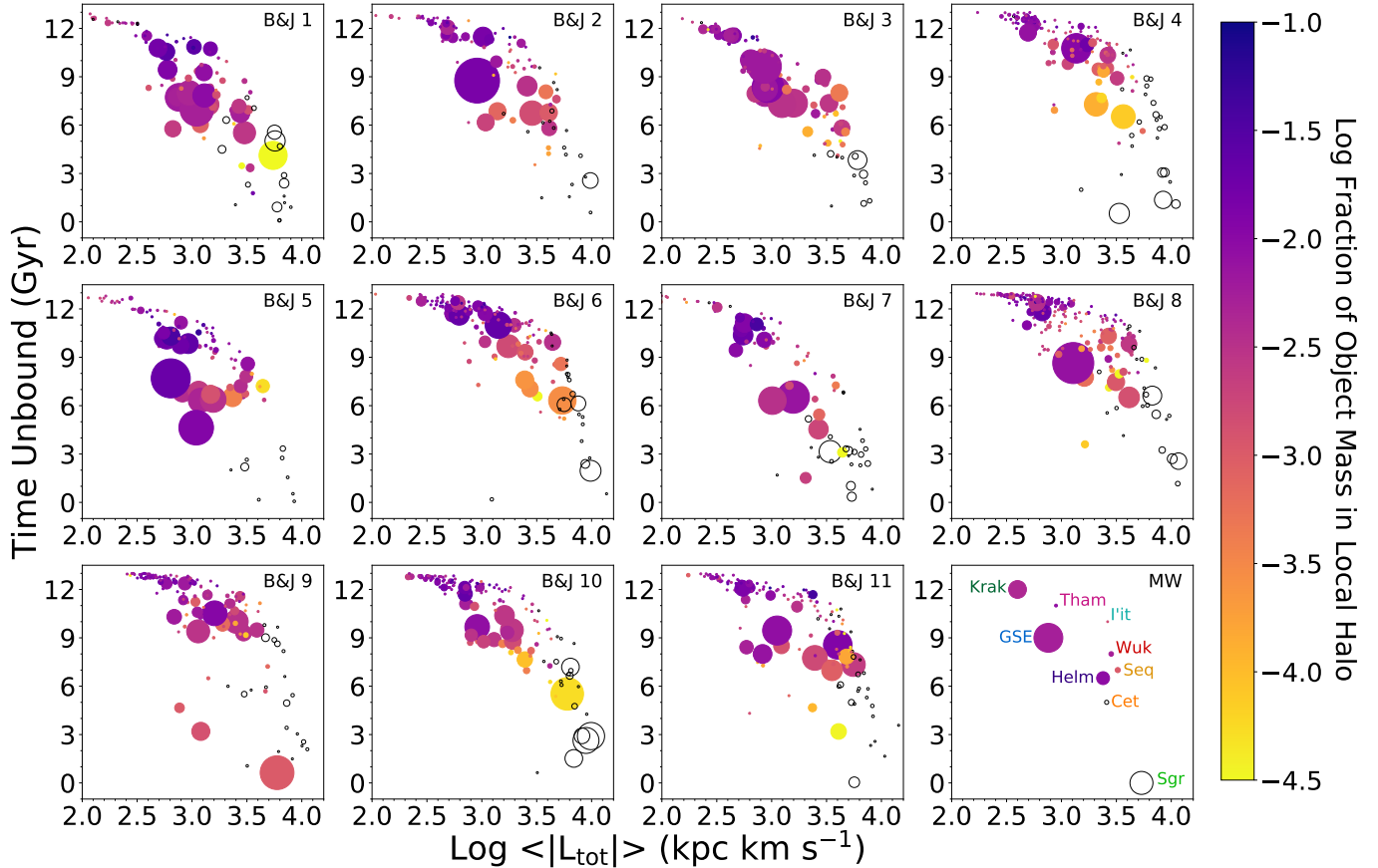


Figure 6. Twelve panels showing properties of disrupted dwarfs from each of the eleven BJ05 Milky Way-like stellar halos that are produced exclusively from dwarf debris, and our composite stellar halo. For each accreted dwarf galaxy, the “time unbound”, or lookback time to when the galaxy ceased to be a gravitationally bound object, is plotted against the logarithm of average angular momentum. Each point, representing a distinct disrupted dwarf galaxy, is colored by the fraction of the object’s mass in the 3 kpc local halo, with black, empty circles having no local halo stars. Circle sizes are proportional to the total object stellar mass to the power 3/4. In the lower right panel, each of the nine halo objects are labeled, with colors consistent to those in Figures 1, 2 and 3. Notice that objects with high angular momentum and more recent times unbound — particularly those with total angular momenta $\gtrsim 4000 \text{ kpc km s}^{-1}$ — generally have low or no solar neighborhood representation. Additionally, objects at very low angular momenta, $\lesssim 300 \text{ kpc km s}^{-1}$ tend to have lower representation than those with moderate angular momenta.

2014; Sanderson et al. 2017; Vasiliev et al. 2021) and dynamic disequilibrium in the Galaxy (e.g., due to the Large Magellanic Cloud; Garavito-Camargo et al. 2019; Conroy et al. 2021; Petersen & Peñarrubia 2021; Erkal et al. 2021; Lilleengen et al. 2022).

To a much lesser extent, dwarfs with very low angular momenta which were accreted very early in the history of the Galaxy ($\gtrsim 12 - 13 \text{ Gyr}$ ago) are also poorly represented in the local halo. For the few accreted dwarfs in this regime which are entirely unrepresented, their debris are concentrated around the galactic center, and therefore beyond the solar neighborhood. However, interestingly a local halo census manages to capture the majority of these most ancient galaxies ingested by the Milky Way.

4. CONCLUSIONS

The overwhelming majority of halo studies rely on solar neighborhood samples. We create a composite Milky Way stellar halo from simulations of the nine most massive disrupted dwarf galaxies to contrast the local halo to the whole halo. Further, we use the eleven stellar halo models built for Milky Way-mass galaxies from BJ05 to place our composite model in context. Our findings are as follows:

1. The local halo does not accurately represent the composition of the stellar halo; some dwarfs are excluded entirely from the sample, while others may be greatly over- or under-represented. [Fig. 3, Sec. 3.2]
2. Extrapolating the properties of the outer halo via orbital integration of local halo stars does not yield an accurate reflection of the outer halo. For

example, the strong retrograde rotation of the outer halo (excluding Sagittarius) is underestimated. This is because the most distant halo stars as well as those with the highest angular momentum do not pass through the solar neighborhood. [Fig. 4 and 5, Sec. 3.2]

3. Comparing with the BJ05 simulations, we find that the chief class of disrupted dwarf galaxies entirely missing from the local halo is comprised of recently accreted systems with high angular momentum (e.g., Cetus). These systems are under-represented in our current census of the halo. [Fig. 6, Sec. 3.3]

In light of the biases discussed in this work, we urge caution when interpreting local halo samples. The composite model presented in this work may already be used as a realistic approximation of the stellar halo to e.g., model survey selection functions. We envision future work will produce self-consistent simulations including boutique models for all dwarfs.

Our findings motivate whole halo samples that both reach to the edge of the Galaxy as well as into the Galactic center – efforts in this spirit include the 2MASS M-giant sample from Majewski et al. 2003, the Pan-STARRS RR Lyrae samples from Sesar et al. 2017; Cohen et al. 2017, and the H3 Survey (Conroy et al. 2019). Upcoming surveys like SDSS-V (Kollmeier et al. 2017), DESI (Allende Prieto et al. 2020), 4MOST (Helmi et al. 2019), and WEAVE (Dalton et al. 2012) promise to re-

veal the most ancient as well as most recent entrants into our Galaxy which are currently missing from our census of disrupted dwarf galaxies.

Software: `Astropy v4.2.1` (Astropy Collaboration et al. 2013, 2018), `gala` (Price-Whelan 2017; Price-Whelan et al. 2018), `jupyter` (Kluyver et al. 2016), `matplotlib` (Hunter 2007), `numpy` (Oliphant 2006--)

We thank Nelson Caldwell for feedback on an early version of this project. We thank Eugene Vasiliev, Vasily Belokurov, and Denis Erkal for their simulation of Sagittarius; Helmer Koppelman, Amina Helmi, Davide Massari, Sebastian Roelenga, and Ulrich Bastian for their simulation of the Helmi Streams; Khyati Malhan, Zhen Yuan, Rodrigo Ibata, Anke Arentsen, Michele Bellazzini, and Nicolas Martin for their simulation of Wukong/LMS-1; Jiang Chang, Zhen Yuan, Xiang-Xiang Xue, Iulia Simion, Xi Kang, Ting Li, Jing-Kun Zhao, and Gang Zhao for their simulation of Cetus; and James Bullock, Kathryn Johnston, Andreea Font, Brant Robertson, and Lars Hernquist for their eleven Milky Way-like stellar halo simulations.

Support for this work was provided by NASA through the NASA Hubble Fellowship grant HST-HF2-51515.001-A awarded by the Space Telescope Science Institute, which is operated by the Association of Universities for Research in Astronomy, Incorporated, under NASA contract NAS5-26555.

REFERENCES

- Aguado, D. S., Belokurov, V., Myeong, G. C., et al. 2021, ApJL, 908, L8, doi: [10.3847/2041-8213/abdbb8](https://doi.org/10.3847/2041-8213/abdbb8)
- Allende Prieto, C., Cooper, A. P., Dey, A., et al. 2020, Research Notes of the American Astronomical Society, 4, 188, doi: [10.3847/2515-5172/abc1dc](https://doi.org/10.3847/2515-5172/abc1dc)
- An, D., & Beers, T. C. 2021, ApJ, 918, 74, doi: [10.3847/1538-4357/ac07a4](https://doi.org/10.3847/1538-4357/ac07a4)
- Astropy Collaboration, Robitaille, T. P., Tollerud, E. J., et al. 2013, A&A, 558, A33, doi: [10.1051/0004-6361/201322068](https://doi.org/10.1051/0004-6361/201322068)
- Astropy Collaboration, Price-Whelan, A. M., Sipőcz, B. M., et al. 2018, AJ, 156, 123, doi: [10.3847/1538-3881/aabc4f](https://doi.org/10.3847/1538-3881/aabc4f)
- Beers, T. C., Carollo, D., Ivezić, Ž., et al. 2012, ApJ, 746, 34, doi: [10.1088/0004-637X/746/1/34](https://doi.org/10.1088/0004-637X/746/1/34)
- Belokurov, V., Erkal, D., Evans, N. W., Koposov, S. E., & Deason, A. J. 2018, MNRAS, 478, 611, doi: [10.1093/mnras/sty982](https://doi.org/10.1093/mnras/sty982)
- Belokurov, V., & Kravtsov, A. 2022, MNRAS, 514, 689, doi: [10.1093/mnras/stac1267](https://doi.org/10.1093/mnras/stac1267)
- Bonaca, A., Geha, M., Küpper, A. H. W., et al. 2014, ApJ, 795, 94, doi: [10.1088/0004-637X/795/1/94](https://doi.org/10.1088/0004-637X/795/1/94)
- Bonaca, A., Conroy, C., Cargile, P. A., et al. 2020, ApJL, 897, L18, doi: [10.3847/2041-8213/ab9caa](https://doi.org/10.3847/2041-8213/ab9caa)
- Bonaca, A., Naidu, R. P., Conroy, C., et al. 2021, ApJL, 909, L26, doi: [10.3847/2041-8213/abeaa9](https://doi.org/10.3847/2041-8213/abeaa9)
- Bovy, J. 2015, ApJS, 216, 29, doi: [10.1088/0067-0049/216/2/29](https://doi.org/10.1088/0067-0049/216/2/29)
- Brown, A. G. A., Velázquez, H. M., & Aguilar, L. A. 2005, MNRAS, 359, 1287, doi: [10.1111/j.1365-2966.2005.09013.x](https://doi.org/10.1111/j.1365-2966.2005.09013.x)
- Buder, S., Lind, K., Ness, M. K., et al. 2022, MNRAS, 510, 2407, doi: [10.1093/mnras/stab3504](https://doi.org/10.1093/mnras/stab3504)
- Bullock, J. S., & Johnston, K. V. 2005, ApJ, 635, 931, doi: [10.1086/497422](https://doi.org/10.1086/497422)
- Carollo, D., Beers, T. C., Lee, Y. S., et al. 2007, Nature, 450, 1020, doi: [10.1038/nature06460](https://doi.org/10.1038/nature06460)
- Carollo, D., Beers, T. C., Chiba, M., et al. 2010, ApJ, 712, 692, doi: [10.1088/0004-637X/712/1/692](https://doi.org/10.1088/0004-637X/712/1/692)

- Chandra, V., Conroy, C., Caldwell, N., et al. 2022, arXiv e-prints, arXiv:2207.13717.
<https://arxiv.org/abs/2207.13717>
- Chang, J., Yuan, Z., Xue, X.-X., et al. 2020, *ApJ*, 905, 100, doi: [10.3847/1538-4357/abc338](https://doi.org/10.3847/1538-4357/abc338)
- Cohen, J. G., Sesar, B., Bahholz, S., et al. 2017, *ApJ*, 849, 150, doi: [10.3847/1538-4357/aa9120](https://doi.org/10.3847/1538-4357/aa9120)
- Conroy, C., Naidu, R. P., Garavito-Camargo, N., et al. 2021, *Nature*, 592, 534, doi: [10.1038/s41586-021-03385-7](https://doi.org/10.1038/s41586-021-03385-7)
- Conroy, C., Bonaca, A., Cargile, P., et al. 2019, *ApJ*, 883, 107, doi: [10.3847/1538-4357/ab38b8](https://doi.org/10.3847/1538-4357/ab38b8)
- Conroy, C., Weinberg, D. H., Naidu, R. P., et al. 2022, arXiv e-prints, arXiv:2204.02989.
<https://arxiv.org/abs/2204.02989>
- Cui, X.-Q., Zhao, Y.-H., Chu, Y.-Q., et al. 2012, *Research in Astronomy and Astrophysics*, 12, 1197, doi: [10.1088/1674-4527/12/9/003](https://doi.org/10.1088/1674-4527/12/9/003)
- Cunningham, E. C., Sanderson, R. E., Johnston, K. V., et al. 2022, *ApJ*, 934, 172, doi: [10.3847/1538-4357/ac78ea](https://doi.org/10.3847/1538-4357/ac78ea)
- Dalton, G., Trager, S. C., Abrams, D. C., et al. 2012, in *Society of Photo-Optical Instrumentation Engineers (SPIE) Conference Series*, Vol. 8446, *Ground-based and Airborne Instrumentation for Astronomy IV*, ed. I. S. McLean, S. K. Ramsay, & H. Takami, 84460P, doi: [10.1117/12.925950](https://doi.org/10.1117/12.925950)
- De Silva, G. M., Freeman, K. C., Bland-Hawthorn, J., et al. 2015, *MNRAS*, 449, 2604, doi: [10.1093/mnras/stv327](https://doi.org/10.1093/mnras/stv327)
- Deason, A. J., Belokurov, V., Koposov, S. E., & Lancaster, L. 2018, *ApJL*, 862, L1, doi: [10.3847/2041-8213/aad0ee](https://doi.org/10.3847/2041-8213/aad0ee)
- Deason, A. J., Belokurov, V., & Sanders, J. L. 2019, *MNRAS*, 490, 3426, doi: [10.1093/mnras/stz2793](https://doi.org/10.1093/mnras/stz2793)
- Deason, A. J., Mao, Y.-Y., & Wechsler, R. H. 2016, *ApJ*, 821, 5, doi: [10.3847/0004-637X/821/1/5](https://doi.org/10.3847/0004-637X/821/1/5)
- Di Matteo, P., Haywood, M., Lehnert, M. D., et al. 2019, *A&A*, 632, A4, doi: [10.1051/0004-6361/201834929](https://doi.org/10.1051/0004-6361/201834929)
- Dodd, E., Callingham, T. M., Helmi, A., et al. 2022, arXiv e-prints, arXiv:2206.11248.
<https://arxiv.org/abs/2206.11248>
- Erkal, D., Deason, A. J., Belokurov, V., et al. 2021, *MNRAS*, 506, 2677, doi: [10.1093/mnras/stab1828](https://doi.org/10.1093/mnras/stab1828)
- Fattahi, A., Belokurov, V., Deason, A. J., et al. 2019, *MNRAS*, 484, 4471, doi: [10.1093/mnras/stz159](https://doi.org/10.1093/mnras/stz159)
- Fattahi, A., Deason, A. J., Frenk, C. S., et al. 2020, *MNRAS*, 497, 4459, doi: [10.1093/mnras/staa2221](https://doi.org/10.1093/mnras/staa2221)
- Feillet, D. K., Sahlholdt, C. L., Feltzing, S., & Casagrande, L. 2021, *MNRAS*, 508, 1489, doi: [10.1093/mnras/stab2614](https://doi.org/10.1093/mnras/stab2614)
- Font, A. S., Johnston, K. V., Bullock, J. S., & Robertson, B. E. 2006, *ApJ*, 646, 886, doi: [10.1086/505131](https://doi.org/10.1086/505131)
- Forbes, D. A. 2020, *MNRAS*, 493, 847, doi: [10.1093/mnras/staa245](https://doi.org/10.1093/mnras/staa245)
- Gaia Collaboration, Brown, A. G. A., Vallenari, A., et al. 2018, ArXiv e-prints. <https://arxiv.org/abs/1804.09365>
- Garavito-Camargo, N., Besla, G., Laporte, C. F. P., et al. 2019, *ApJ*, 884, 51, doi: [10.3847/1538-4357/ab32eb](https://doi.org/10.3847/1538-4357/ab32eb)
- Gómez, F. A., Helmi, A., Cooper, A. P., et al. 2013, *MNRAS*, 436, 3602, doi: [10.1093/mnras/stt1838](https://doi.org/10.1093/mnras/stt1838)
- Han, J. J., Conroy, C., Johnson, B. D., et al. 2022, arXiv e-prints, arXiv:2208.04327.
<https://arxiv.org/abs/2208.04327>
- Haywood, M., Di Matteo, P., Lehnert, M. D., et al. 2018, *ApJ*, 863, 113, doi: [10.3847/1538-4357/aad235](https://doi.org/10.3847/1538-4357/aad235)
- Helmi, A. 2020, *ARA&A*, 58, 205, doi: [10.1146/annurev-astro-032620-021917](https://doi.org/10.1146/annurev-astro-032620-021917)
- Helmi, A., Babusiaux, C., Koppelman, H. H., et al. 2018, *Nature*, 563, 85, doi: [10.1038/s41586-018-0625-x](https://doi.org/10.1038/s41586-018-0625-x)
- Helmi, A., Veljanoski, J., Breddels, M. A., Tian, H., & Sales, L. V. 2017, *A&A*, 598, A58, doi: [10.1051/0004-6361/201629990](https://doi.org/10.1051/0004-6361/201629990)
- Helmi, A., White, S. D. M., de Zeeuw, P. T., & Zhao, H. 1999, *Nature*, 402, 53, doi: [10.1038/46980](https://doi.org/10.1038/46980)
- Helmi, A., Irwin, M., Deason, A., et al. 2019, *The Messenger*, 175, 23, doi: [10.18727/0722-6691/5120](https://doi.org/10.18727/0722-6691/5120)
- Horta, D., Schiavon, R. P., Mackereth, J. T., et al. 2021, *MNRAS*, 500, 1385, doi: [10.1093/mnras/staa2987](https://doi.org/10.1093/mnras/staa2987)
- Hunter, J. D. 2007, *Computing In Science & Engineering*, 9, 90, doi: [10.1109/MCSE.2007.55](https://doi.org/10.1109/MCSE.2007.55)
- Ibata, R. A., Gilmore, G., & Irwin, M. J. 1994, *Nature*, 370, 194, doi: [10.1038/370194a0](https://doi.org/10.1038/370194a0)
- Jean-Baptiste, I., Di Matteo, P., Haywood, M., et al. 2017, *A&A*, 604, A106, doi: [10.1051/0004-6361/201629691](https://doi.org/10.1051/0004-6361/201629691)
- Ji, A. P., Li, T. S., Hansen, T. T., et al. 2020, *AJ*, 160, 181, doi: [10.3847/1538-3881/abacb6](https://doi.org/10.3847/1538-3881/abacb6)
- Johnson, B. D., Conroy, C., Naidu, R. P., et al. 2020, *ApJ*, 900, 103, doi: [10.3847/1538-4357/abab08](https://doi.org/10.3847/1538-4357/abab08)
- Kluyver, T., Ragan-Kelley, B., Pérez, F., et al. 2016, in *Positioning and Power in Academic Publishing: Players, Agents and Agendas*, ed. F. Loizides & B. Schmidt, IOS Press, 87 – 90
- Kollmeier, J. A., Zasowski, G., Rix, H.-W., et al. 2017, arXiv e-prints, arXiv:1711.03234.
<https://arxiv.org/abs/1711.03234>
- Koppelman, H. H., Helmi, A., Massari, D., Roelenga, S., & Bastian, U. 2019, *A&A*, 625, A5, doi: [10.1051/0004-6361/201834769](https://doi.org/10.1051/0004-6361/201834769)
- Kruijssen, J. M. D., Pfeffer, J. L., Reina-Campos, M., Crain, R. A., & Bastian, N. 2019, *MNRAS*, 486, 3180, doi: [10.1093/mnras/sty1609](https://doi.org/10.1093/mnras/sty1609)

- Kruijssen, J. M. D., Pfeffer, J. L., Chevance, M., et al. 2020, *MNRAS*, 498, 2472, doi: [10.1093/mnras/staa2452](https://doi.org/10.1093/mnras/staa2452)
- Law, D. R., & Majewski, S. R. 2010, *ApJ*, 714, 229, doi: [10.1088/0004-637X/714/1/229](https://doi.org/10.1088/0004-637X/714/1/229)
- Lee, D. M., Johnston, K. V., Sen, B., & Jessop, W. 2015, *ApJ*, 802, 48, doi: [10.1088/0004-637X/802/1/48](https://doi.org/10.1088/0004-637X/802/1/48)
- Lilleengen, S., Petersen, M. S., Erkal, D., et al. 2022, arXiv e-prints, arXiv:2205.01688. <https://arxiv.org/abs/2205.01688>
- Limberg, G., Santucci, R. M., Rossi, S., et al. 2021, *ApJL*, 913, L28, doi: [10.3847/2041-8213/ac0056](https://doi.org/10.3847/2041-8213/ac0056)
- Mackereth, J. T., & Bovy, J. 2020, *MNRAS*, 492, 3631, doi: [10.1093/mnras/staa047](https://doi.org/10.1093/mnras/staa047)
- Majewski, S. R., Skrutskie, M. F., Weinberg, M. D., & Ostheimer, J. C. 2003, *ApJ*, 599, 1082, doi: [10.1086/379504](https://doi.org/10.1086/379504)
- Majewski, S. R., Schiavon, R. P., Frinchaboy, P. M., et al. 2017, *AJ*, 154, 94, doi: [10.3847/1538-3881/aa784d](https://doi.org/10.3847/1538-3881/aa784d)
- Malhan, K., Yuan, Z., Ibata, R. A., et al. 2021, *ApJ*, 920, 51, doi: [10.3847/1538-4357/ac1675](https://doi.org/10.3847/1538-4357/ac1675)
- Malhan, K., Ibata, R. A., Sharma, S., et al. 2022, *ApJ*, 926, 107, doi: [10.3847/1538-4357/ac4d2a](https://doi.org/10.3847/1538-4357/ac4d2a)
- Massari, D., Koppelman, H. H., & Helmi, A. 2019, *A&A*, 630, L4, doi: [10.1051/0004-6361/201936135](https://doi.org/10.1051/0004-6361/201936135)
- Matsuno, T., Aoki, W., & Suda, T. 2019, *ApJL*, 874, L35, doi: [10.3847/2041-8213/ab0ec0](https://doi.org/10.3847/2041-8213/ab0ec0)
- Matsuno, T., Koppelman, H. H., Helmi, A., et al. 2021, arXiv e-prints, arXiv:2111.15423. <https://arxiv.org/abs/2111.15423>
- Matsuno, T., Dodd, E., Koppelman, H. H., et al. 2022, *A&A*, 665, A46, doi: [10.1051/0004-6361/202243609](https://doi.org/10.1051/0004-6361/202243609)
- Monty, S., Venn, K. A., Lane, J. M. M., Lokhorst, D., & Yong, D. 2020, *MNRAS*, 497, 1236, doi: [10.1093/mnras/staa1995](https://doi.org/10.1093/mnras/staa1995)
- Myeong, G. C., Belokurov, V., Aguado, D. S., et al. 2022, *ApJ*, 938, 21, doi: [10.3847/1538-4357/ac8d68](https://doi.org/10.3847/1538-4357/ac8d68)
- Myeong, G. C., Vasiliev, E., Iorio, G., Evans, N. W., & Belokurov, V. 2019, *MNRAS*, 488, 1235, doi: [10.1093/mnras/stz1770](https://doi.org/10.1093/mnras/stz1770)
- Naidu, R. P., Conroy, C., Bonaca, A., et al. 2020, *ApJ*, 901, 48, doi: [10.3847/1538-4357/abaef4](https://doi.org/10.3847/1538-4357/abaef4)
- . 2021, *ApJ*, 923, 92, doi: [10.3847/1538-4357/ac2d2d](https://doi.org/10.3847/1538-4357/ac2d2d)
- . 2022a, arXiv e-prints, arXiv:2204.09057. <https://arxiv.org/abs/2204.09057>
- Naidu, R. P., Ji, A. P., Conroy, C., et al. 2022b, *ApJL*, 926, L36, doi: [10.3847/2041-8213/ac5589](https://doi.org/10.3847/2041-8213/ac5589)
- Newberg, H. J., Yanny, B., & Willett, B. A. 2009, *ApJL*, 700, L61, doi: [10.1088/0004-637X/700/2/L61](https://doi.org/10.1088/0004-637X/700/2/L61)
- Oliphant, T. 2006–, NumPy: A guide to NumPy, USA: Trelgol Publishing. <http://www.numpy.org/>
- Petersen, M. S., & Peñarrubia, J. 2021, *Nature Astronomy*, 5, 251, doi: [10.1038/s41550-020-01254-3](https://doi.org/10.1038/s41550-020-01254-3)
- Pfeffer, J., Lardo, C., Bastian, N., Saracino, S., & Kamann, S. 2021, *MNRAS*, 500, 2514, doi: [10.1093/mnras/staa3407](https://doi.org/10.1093/mnras/staa3407)
- Price-Whelan, A. M. 2017, *The Journal of Open Source Software*, 2, doi: [10.21105/joss.00388](https://doi.org/10.21105/joss.00388)
- Price-Whelan, A. M., Sipőcz, B. M., Günther, H. M., et al. 2018, *AJ*, 156, 123, doi: [10.3847/1538-3881/aabc4f](https://doi.org/10.3847/1538-3881/aabc4f)
- Rix, H.-W., Chandra, V., Andrae, R., et al. 2022, arXiv e-prints, arXiv:2209.02722. <https://arxiv.org/abs/2209.02722>
- Robertson, B., Bullock, J. S., Font, A. S., Johnston, K. V., & Hernquist, L. 2005, *ApJ*, 632, 872, doi: [10.1086/452619](https://doi.org/10.1086/452619)
- Ruiz-Lara, T., Matsuno, T., Sofie Lövdal, S., et al. 2022, arXiv e-prints, arXiv:2201.02405. <https://arxiv.org/abs/2201.02405>
- Sanderson, R. E., Hartke, J., & Helmi, A. 2017, *ApJ*, 836, 234, doi: [10.3847/1538-4357/aa5eb4](https://doi.org/10.3847/1538-4357/aa5eb4)
- Schönrich, R., Asplund, M., & Casagrande, L. 2011, *MNRAS*, 415, 3807, doi: [10.1111/j.1365-2966.2011.19003.x](https://doi.org/10.1111/j.1365-2966.2011.19003.x)
- Sesar, B., Hernitschek, N., Mitrović, S., et al. 2017, *AJ*, 153, 204, doi: [10.3847/1538-3881/aa661b](https://doi.org/10.3847/1538-3881/aa661b)
- Shank, D., Komater, D., Beers, T. C., Placco, V. M., & Huang, Y. 2022, arXiv e-prints, arXiv:2201.08337. <https://arxiv.org/abs/2201.08337>
- Shipp, N., Drlica-Wagner, A., Balbinot, E., et al. 2018, *ApJ*, 862, 114, doi: [10.3847/1538-4357/aacdab](https://doi.org/10.3847/1538-4357/aacdab)
- Simpson, C. M., Gargiulo, I., Gómez, F. A., et al. 2019, *MNRAS*, 490, L32, doi: [10.1093/mnrasl/slz142](https://doi.org/10.1093/mnrasl/slz142)
- Sofie Lövdal, S., Ruiz-Lara, T., Koppelman, H. H., et al. 2022, arXiv e-prints, arXiv:2201.02404. <https://arxiv.org/abs/2201.02404>
- Steinmetz, M., Zwitter, T., Siebert, A., et al. 2006, *AJ*, 132, 1645, doi: [10.1086/506564](https://doi.org/10.1086/506564)
- Tenachi, W., Oria, P.-A., Ibata, R., et al. 2022, arXiv e-prints, arXiv:2206.10405. <https://arxiv.org/abs/2206.10405>
- Thomas, G. F., & Battaglia, G. 2021, arXiv e-prints, arXiv:2112.03973. <https://arxiv.org/abs/2112.03973>
- Vasiliev, E., Belokurov, V., & Erkal, D. 2021, *MNRAS*, 501, 2279, doi: [10.1093/mnras/staa3673](https://doi.org/10.1093/mnras/staa3673)
- White, S. D. M., & Frenk, C. S. 1991, *ApJ*, 379, 52, doi: [10.1086/170483](https://doi.org/10.1086/170483)
- Yanny, B., Rockosi, C., Newberg, H. J., et al. 2009, *AJ*, 137, 4377, doi: [10.1088/0004-6256/137/5/4377](https://doi.org/10.1088/0004-6256/137/5/4377)
- Yuan, Z., Chang, J., Beers, T. C., & Huang, Y. 2020, *ApJL*, 898, L37, doi: [10.3847/2041-8213/aba49f](https://doi.org/10.3847/2041-8213/aba49f)

Yuan, Z., Malhan, K., Sestito, F., et al. 2021, arXiv e-prints, arXiv:2112.05775.
<https://arxiv.org/abs/2112.05775>